MOLECULAR AND CELLULAR BIOLOGY, Oct. 2007, p. 7188–7197 Vol. 27, No. 20
0270-7306/07/$08.00+0 doi:10.1128/MCB.00915-07


# NRF2 Modulates Aryl Hydrocarbon Receptor Signaling: Influence on Adipogenesis▽†

Soona Shin,[1] Nobunao Wakabayashi,[2] Vikas Misra,[2] Shyam Biswal,[2] Gum Hwa Lee,[2] Elin S. Agoston,[1] Masayuki Yamamoto,[3] and Thomas W. Kensler[1,2]*

*Department of Pharmacology and Molecular Sciences, School of Medicine,[1] and Department of Environmental Health Sciences, Bloomberg School of Public Health,[2] The Johns Hopkins University, Baltimore, Maryland 21205, and Institute of Basic Medical Sciences and Center for Tsukuba Advanced Research Alliance, University of Tsukuba, Tennoudai, Tsukuba 305-8577, Japan[3]*

Received 23 May 2007/Returned for modification 29 June 2007/Accepted 8 August 2007

**The NF-E2 p45-related factor 2 (NRF2) and the aryl hydrocarbon receptor (AHR) are transcription factors controlling pathways modulating xenobiotic metabolism. AHR has recently been shown to affect *Nrf2* expression. Conversely, this study demonstrates that NRF2 regulates expression of *Ahr* and subsequently modulates several downstream events of the AHR signaling cascade, including (i) transcriptional control of the xenobiotic metabolism genes *Cyp1a1* and *Cyp1b1* and (ii) inhibition of adipogenesis in mouse embryonic fibroblasts (MEFs). Constitutive expression of AHR was affected by *Nrf2* genotype. Moreover, a pharmacological activator of NRF2 signaling, CDDO-IM {1-[2-cyano-3,12-dioxooleana-1,9(11)-dien-28-oyl]imidazole}, induced *Ahr*, *Cyp1a1*, and *Cyp1b1* transcription in $Nrf2^{+/+}$ MEFs but not in $Nrf2^{-/-}$ MEFs. Reporter analysis and chromatin immunoprecipitation assay revealed that NRF2 directly binds to one antioxidant response element (ARE) found in the −230-bp region of the promoter of *Ahr*. Since AHR negatively controls adipocyte differentiation, we postulated that NRF2 would inhibit adipogenesis through the interaction with the AHR pathway. $Nrf2^{-/-}$ MEFs showed markedly accelerated adipogenesis upon stimulation, while $Keap1^{-/-}$ MEFs (which exhibit higher NRF2 signaling) differentiated slowly compared to their congenic wild-type MEFs. Ectopic expression of *Ahr* and dominant-positive *Nrf2* in $Nrf2^{-/-}$ MEFs also substantially delayed differentiation. Thus, NRF2 directly modulates AHR signaling, highlighting bidirectional interactions of these pathways.**

NRF2 is a cap'n'collar (CNC) basic leucine zipper (bZIP) transcription factor and an important regulator of the transcription of cytoprotective enzymes and antioxidant genes, such as glutathione *S*-transferases (GSTs) and NAD(P)H (quinone acceptor) oxidoreductase 1 (NQO1), through binding to antioxidant response elements (AREs) found in their promoters (20, 28). The NRF2 pathway can be modulated in a dynamic way by multiple pharmacological agents {NRF2 activators, including 1-[2-cyano-3,12-dioxooleana-1,9(11)-dien-28-oyl]imidazole (CDDO-Im)} through interactions with KEAP1, a cytoplasmic binding partner of NRF2 (12, 50, 51). Studies using *Nrf2* and *Keap1* knockout mice have provided key insights into the importance of this pathway in protecting cells from exposure to environmental toxins, inflammatory stresses, neurodegeneration, and carcinogenesis (18). Although more resistant to toxins (32), *Keap1* null mice, which have higher constitutive levels of NRF2, showed hyperkeratosis, which implies that the pathway may also be involved in keratinocyte differentiation (46).

Information generated from analyses of genetic networks and large-scale two-hybrid screens has indicated that to understand the complexity of a phenotype or disease, one needs to investigate the interplay of signals and transcription factors that leads to the expression of downstream genes (3, 24). Although much is known about the role of the NRF2 pathway itself, little is known about its interaction with other signaling pathways. Recent evidence suggests that cross talk may exist between aryl hydrocarbon receptor (AHR) and NRF2 pathways. AHR is a ligand-activated transcription factor that belongs to the basic helix-loop-helix/PER-aryl hydrocarbon receptor nuclear translocator (ARNT)-SIM family. When activated by a ligand, AHR translocates to the nucleus and dimerizes with ARNT, another basic helix-loop-helix protein. AHR is activated when bound with ligand, usually a planar polyaromatic chemical. Activated AHR then binds to xenobiotic response elements (XREs) in the promoters of various cytochrome P450s (CYPs) (1, 15), resulting in increased expression of these enzymes. Because several AHR ligands are suspected carcinogens, such as 2,3,7,8-tetrachlorodibenzo-*p*-dioxin (TCDD) and benzo[*a*]pyrene, the majority of studies on AHR have focused on its role in mediating the toxicity of these chemicals. However, studies utilizing *Ahr* knockout mice and cell lines revealed that AHR signaling may be involved also in physiological processes, such as growth and differentiation, in a manner that is independent of exogenous ligand (2, 34). Moreover, it has been reported that the AHR pathway is involved in maintaining a balance between promoting and preventing oxidative stress as well as in preventing toxic redox cycles of catechol estrogens (21, 29). AHR also regulates gene expression involved in cytoskeletal organization, bioenergetics, and cell proliferation (9). Several studies suggest that one of the physiological roles of the AHR is the negative regulation of

* Corresponding author. Mailing address: Department of Environmental Health Sciences, Bloomberg School of Public Health, Room E7541, The Johns Hopkins University, Baltimore, MD 21205. Phone: (410) 955-4712. Fax: (410) 955-0116. E-mail: tkensler@jhsph.edu.

† Supplemental material for this article may be found at http://mcb.asm.org/.

▽ Published ahead of print on 20 August 2007.

adipocyte differentiation. Shimba et al. (41) have demonstrated that TCDD treatment suppresses the conversion of 3T3-L1 cells into adipocytes. Using MEF cell lines derived from *Ahr* knockout mice, Alexander et al. (2) reported that the AHR is a constitutive inhibitor of triglyceride synthesis and an early regulator of adipocyte differentiation. In addition, one of the phenotypes of *Ahr* null mice is transient fatty liver (39), implying an in vivo regulatory role of AHR in the adipogenic process.

Studies on cross talk between AHR and NRF2 have focused on their roles in controlling expression of xenobiotic-metabolizing enzymes. For example, it has been reported that the inducible expression of NQO1 by TCDD depends on both AHR and NRF2 (25). Miao et al. (27) demonstrated that *Nrf2* gene transcription is directly modulated by AHR activation. The present study demonstrates that signaling in the opposite direction also occurs, namely, that transcription of the *Ahr* gene is directly affected by NRF2. Our data clearly demonstrate that expression of *Ahr*, *Cyp1a1*, and *Cyp1b1* is partially dependent on NRF2, implying that NRF2 modulates both transcription of *Ahr* and its downstream targets. In addition, our results indicate that the NRF2 pathway inhibits adipogenesis via activation of the AHR signaling cascade. Thus, the NRF2 pathway has a broader reach than heretofore described, i.e., indirect regulation of the expression of CYPs, inhibition of adipogenesis, and possibly other AHR-dependent processes.

## MATERIALS AND METHODS

**Cell culture.** Immortalized mouse embryonic fibroblasts (MEFs) were established from the embryos of C57BL/6J *Nrf2*$^{-/-}$ or *Nrf2*$^{+/+}$ littermates. Primary MEFs were established from the embryos of *Keap1*$^{-/-}$ or *Keap1*$^{+/+}$ littermates. The cells were cultured in Iscove's minimal essential medium (Invitrogen) containing 10% fetal bovine serum (Invitrogen) and incubated at 37°C in a humidified atmosphere of 5% $CO_2$.

**Plasmids.** The mouse *Ahr* gene regulatory region was isolated from C57BL/6J mouse liver genomic DNA by PCR. The region was directly cloned between KpnI and NcoI sites in pGL3-Basic (Promega) and confirmed by sequencing analysis. In this construct, ATG of AHR was fused to that of luciferase. Serial promoter deletion fragments were prepared by the S1 exonuclease III nuclease reaction method followed by NcoI digestion. Then, the fragments were ligated to the site between KpnI and NcoI sites of pGL3 basic. The mutant ARE reporter was produced by ligating oligonucleotide containing the mutated ARE (GGTACCCACTACGTCCTCCGTCCAACCGTGCTGCGAAG AGGGTGGGGCC) to the site between KpnI and ApaI of p-967 construct. All constructs were confirmed by sequencing. Because pRLTK (Promega) bears an ARE in the thymidine kinase (TK) promoter region, this ARE was deleted in order to use this vector for normalizing transfection efficiency. This improved normalizing vector, pRLTK-ΔARE, was constructed by deleting the SmaI and PvuII fragment from pRLTK. Constructs used in transfection experiments were purified with QIAGEN plasmid kits. For establishment of stable transfectants, cDNAs for murine *Ahr* and *Nrf2*ΔNeh2 were inserted into pTracer-EF/Bsd (Invitrogen). *Ahr* cDNA was isolated from pSportAHR (ATCC 63125). *Nrf2*ΔNeh2 cDNA (17) was isolated from pcDNA3-*Nrf2*ΔNeh2 (generously provided by Ken Itoh, Hirosaki University).

**Transient transfection and measurement of luciferase activity.** Cells were transfected at 60 to 70% confluence with GeneJuice transfection reagent (Novagen). Briefly, cells were seeded in 24-well plates at a density of $1 \times 10^4$ cells/well. Cells were grown overnight; the transfection complex containing 0.45 μg of plasmid DNA, 0.05 μg of the pRLTK-ΔARE plasmid, and transfection reagent was added to each well, and cells were incubated for 15 h. Cells were then incubated for another 24 h with or without drug treatment. *Renilla* and firefly luciferase activities in cell lysates were measured with the Dual Luciferase assay kit (Promega) with a luminometer (Turner Designs). For forced expression studies, pcDNA3-*Nrf2*ΔNeh2 was cotransfected with promoter plasmids.

**Isolation and purification of total RNA and RT-PCR.** Cells were seeded at 60% confluence the day before treatment with vehicle or CDDO-Im. Total RNA was purified using the Versagene RNA purification system (Gentra Systems). Genes were analyzed by SYBR green real-time quantitative reverse transcription-PCR (RT-PCR). cDNA was synthesized using the iScript system (Bio-Rad). Real-time PCR was performed on a Bio-Rad My-IQ real-time PCR instrument using Applied Biosystems SYBR green PCR master mix in 20-μl reaction mixture volumes. The PCR efficiency was determined from a standard curve and used in the Pfaffl method for calculation of relative quantification (33). Tata-binding protein (*Tbp*) was used as a normalizing control. Primers are shown in Table S1 in the supplemental material.

**Chromatin immunoprecipitation (ChIP) assay.** Formaldehyde cross-linking and chromatin fragmentation were carried out as described previously (22). Diluted chromatin solution was incubated with an anti-NRF2 antibody or nonspecific immunoglobulin G (Santa Cruz Biotechnology) for 18 h at 4°C with rotation. After the DNA was washed and eluted, precipitated DNA was resuspended with 60 μl of water, and 2 μl of DNA was used for PCR amplification with the following primers for *Ahr* ARE, 5′-TTTTGAGGCTGGAAAACAGG TACT-3′ and 5′-ACGTGATGACGCAGGACGTA-3′. The primer sequences for promoters of β-*actin* and *Gsta1* ARE have been described previously (22).

**Design and transfection of *Ahr*-targeted specific siRNA.** Small interfering RNA (siRNA) duplexes were prepared by Ambion. Targeted coding regions of the *Ahr* oligonucleotide sequences were as follows: iAhr (5′-AAGACTGGAG AAAGTGGCATG-3′) (13) and iAhr2 (5′-AACGAGGAGTTCTTCAGAACT-3′) (predesigned by Ambion). A National Center for Biotechnology Information standard nucleotide-nucleotide BLAST program was used to verify that this sequence did not match that of any other mouse gene. Quantitative RT-PCR results confirmed that transfection with iAhr reduced mRNA levels of *Ahr* more efficiently than transfection with iAhr2 did; therefore, iAhr was used for subsequent experiments. The negative-control siRNA (AM4611) used in this study was a nonsilencing siRNA designed by Ambion. MEFs were seeded in a six-well plate and transfected in the presence of 30 nM of either siRNA or negative-control RNA in a final volume of 1 ml OPTI-MEM (Invitrogen) with Lipofectamine 2000 (Invitrogen). After 24 h, cells were replenished with fresh culture medium containing 10% fetal bovine serum (FBS). Cells were incubated for an additional 40 h, and extracted RNA and proteins were analyzed by RT-PCR and immunoblotting.

**Protein isolation and immunoblots.** MEFs were lysed in the Tris-HCl buffer (10 mM, pH 7.5), 1% NP-40, 0.1% sodium deoxycholate, 0.1% sodium dodecyl sulfate, 150 mM sodium chloride, and 1 mM EDTA for 30 min at 4°C. The samples were centrifuged at $10{,}000 \times g$ for 10 min to pellet debris. Cell lysates were loaded and run on a 8% sodium dodecyl sulfate-polyacrylamide gel before being transferred electrophoretically onto a polyvinylidene difluoride membrane. The membrane was blocked with 5% fat-free milk solution and then sequentially incubated with primary antibody and enzyme-conjugated secondary antibody. The results were documented on X-ray film by using an ECL detection kit (Amersham Biosciences). Immunoblot analysis confirmed the expression of AHR and NRF2ΔNeh2 in the stable clones (data not shown) using anti-AHR antibody (Biomol) and anti-NRF2 antibody (generously provided by Ken Itoh, Hirosaki University). Polyclonal anti-β-actin antibody and anti-lamin B antibody were obtained from Santa Cruz Biotechnology.

**Induction of differentiation.** A protocol for adipocyte differentiation of MEFs was used as described previously (2). Briefly, MEFs were plated at a 100% confluence in a 12-well plate 24 to 48 h before stimulation of differentiation. For the first 3 days, cells were maintained in Dulbecco modified Eagle medium (DMEM) supplemented with 10% FBS, 10 μg/ml insulin (Sigma), 5 μM dexamethasone (Sigma), 0.2 mM isobutylmethylxanthine (Sigma), and 1 μM rosiglitazone (Cayman Chemical) for the first 3 days. Subsequently, cells were maintained in DMEM supplemented with 10% FBS, 10 μg/ml insulin, and 1 μM rosiglitazone. Oil Red O staining was done per the manufacturer's instructions (Chemicon).

## RESULTS

**AHR expression and signaling are regulated by NRF2 in murine embryonic fibroblasts.** Microarray analyses of MEFs derived from *Nrf2*$^{+/+}$ and *Nrf2*$^{-/-}$ mice have been conducted to compare the influence of the transcription factor genotype on global gene expression patterns (data not shown). These studies suggested that NRF2 may affect expression levels of *Ahr* and some of its downstream target genes. To follow up on this observation, a more direct analysis was undertaken in the

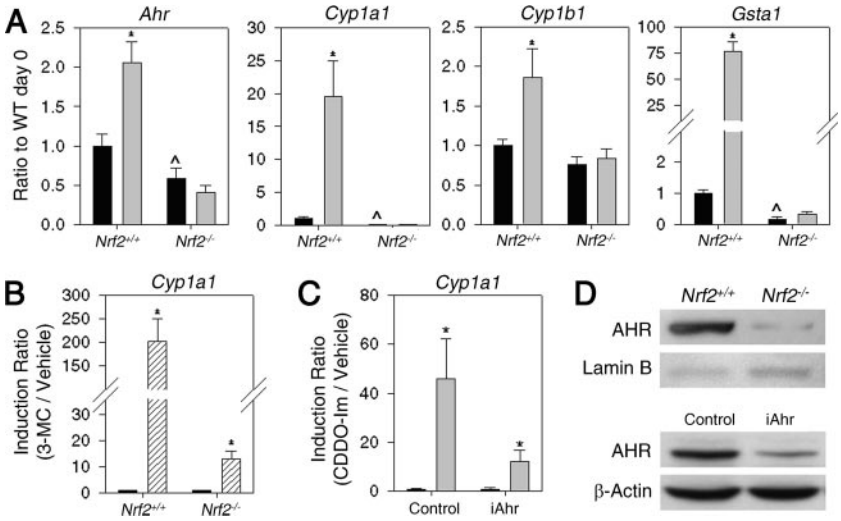


FIG. 1. Differential expression analysis of *Ahr* and downstream genes in $Nrf2^{+/+}$ and $Nrf2^{-/-}$ MEFs. (A) Transcript levels were measured following treatment with vehicle (black bars) and 25 nM CDDO-Im (gray bars) for 24 h. Ratios to $Nrf2^{+/+}$ vehicle-treated controls on day 0 (Ratio to WT day 0) are shown on the *y* axes. Values are means plus standard errors (SEs) (error bars) ($n = 4$). Values that are significantly different ($P < 0.05$) from that of the respective vehicle (*) or that of the wild-type vehicle (WT) (^) are indicated. (B) Transcript levels were measured following treatment with vehicle (black bar) and 2 μM 3-MC (hatched bar) for 24 h. Ratios to the respective vehicle-treated control (Induction Ratio) are shown. Values are means plus SEs (error bars) ($n = 3$). Values that are significantly different ($P < 0.05$) from that of the respective vehicle (*) are indicated. (C) MEF cells were transfected with 30 nM siRNA (iAhr) or control RNA. Cells were treated with 25 nM CDDO-Im for 24 h or vehicle. Ratios to the respective vehicle-treated control (Induction Ratio) are shown. Values are means plus SEs (error bars) ($n = 4$). Values that are significantly different ($P < 0.05$) from that of the respective vehicle (*) are indicated. (D) Protein levels of AHR were detected by immunoblotting. (Top blots) AHR protein levels in $Nrf2^{+/+}$ and $Nrf2^{-/-}$ MEFs. (Bottom blots) AHR protein levels in control and iAhr-treated $Nrf2^{+/+}$ MEFs.

present study. Both mRNA and protein levels of AHR were higher in $Nrf2^{+/+}$ MEFs than in $Nrf2^{-/-}$ MEFs (Fig. 1A and D). Quantitative RT-PCR indicated that constitutive expression of AHR target gene *Cyp1a1*, but not *Cyp1b1*, was significantly lower in $Nrf2^{-/-}$ MEFs (Fig. 1A). The mRNA levels of *Ahr* were elevated 2.1-fold by CDDO-Im, a potent activator of NRF2 signaling, in $Nrf2^{+/+}$ MEFs but not in $Nrf2^{-/-}$ MEFs. The mRNA levels of *Arnt*, which encodes a heterodimeric binding partner of AHR, were not affected by *Nrf2* genotype or CDDO-Im (data not shown). CDDO-Im induced transcription of AHR target genes *Cyp1a1* and *Cyp1b1* in $Nrf2^{+/+}$ MEFs but not in $Nrf2^{-/-}$ MEFs, implying that the NRF2 pathway influences the transcriptional function of AHR. *Gsta1*, a well-characterized NRF2-regulated gene, was induced over 75-fold in $Nrf2^{+/+}$ MEFs but not at all in $Nrf2^{-/-}$ MEFs.

Cells were treated with siRNA for *Ahr* (iAhr) to determine whether CDDO-Im induces *Cyp1a1* transcription through the AHR pathway. Treatment with iAhr resulted in a 70 to 80% knockdown of AHR protein (Fig. 1D). After transfection with iAhr, induction of *Cyp1a1* transcripts by CDDO-Im was only 25% of that observed in AHR-intact control cells (Fig. 1C). To test whether there is any off-target effect, mRNA levels of β-*actin* and hypoxanthine-guanine phosphoribosyltransferase (*Hprt*) were measured using quantitative RT-PCR. Transfection of iAhr had no effect on these genes (data not shown), confirming the specificity of the siRNA construct.

The fact that mRNA levels of *Ahr* are lower in $Nrf2^{-/-}$ MEFs than in $Nrf2^{+/+}$ MEFs suggests that the response to AHR ligands may be impaired in $Nrf2^{-/-}$ MEFs. To determine whether the AHR-XRE pathway is intact in $Nrf2^{-/-}$ MEFs, 3-methylcholanthrene (3-MC), a prototypical ligand that directly binds to AHR, was used. In $Nrf2^{+/+}$ MEFs, the mRNA levels of *Cyp1a1* were increased by 200-fold by 2 μM 3-MC (Fig. 1B). In $Nrf2^{-/-}$ MEFs, the drug treatment resulted in 13-fold induction of *Cyp1a1*, suggesting that enhancement of AHR signaling by AHR agonists is suppressed in $Nrf2^{-/-}$ MEFs.

**Transcription of the *Ahr* gene is regulated by an ARE located in its proximal promoter.** To analyze the regulation of *Ahr* by NRF2, the promoter region (−967 bp upstream of the transcription start site) was isolated from mouse liver genomic DNA by PCR amplification and ligated into the luciferase reporter pGL3 basic vector. Three potential AREs were identified by consensus sequence: one upstream of the transcription start site (−230 bp) and two downstream (185 bp and 396 bp) of the putative poly(A) addition signal (Fig. 2A).

The reporter construct with the promoter of the *Ahr* gene (p-967) showed higher basal luciferase activity (data not shown) and inducible luciferase activity than the construct with both promoter and downstream enhancer sequences (p-967/560) (Fig. 2B). These data suggest that the two AREs in the downstream region are not involved in NRF2-AHR cross regulation. To determine the location of the *cis* element(s) involved in this cross regulation, two truncated promoter constructs were made (p-242 and p-193). Wild-type MEFs were transfected with these constructs, and luciferase activities from transfected cells following CDDO-Im treatment or forced expression of *Nrf2*ΔNeh2 were measured. Neh2 is the negative regulatory domain of NRF2 that is involved with the interaction with KEAP1 (17, 19). The plasmid *Nrf2*ΔNeh2 expresses a dominant-positive form of NRF2 protein that is more resistant to proteosomal degradation than the wild-type protein is. The

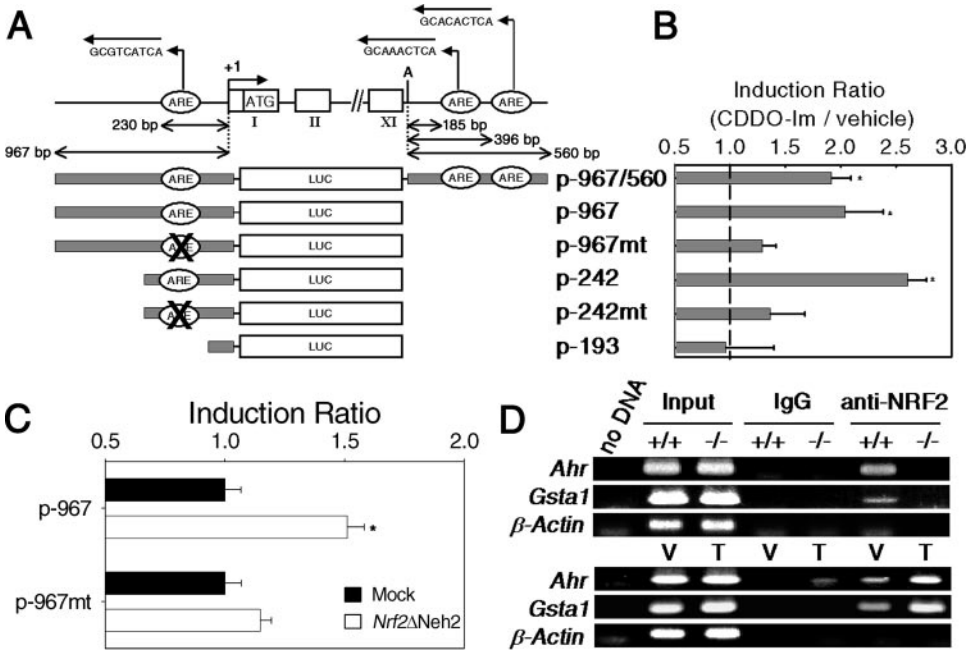


FIG. 2. Analysis of murine *Ahr* promoter. (A) Murine *Ahr* promoter constructs are shown. Three AREs in an inverted direction were identified, one upstream of the transcription start site (labeled "+1") and two downstream of the putative poly(A) addition signal (labeled "A") of the *Ahr* gene. Arrows indicate the orientations of these putative AREs. Boxes marked with roman numerals indicate exons of the murine *Ahr* promoter. LUC, luciferase. (B) Luciferase activities derived from full-length, truncated, or mutated promoters following treatment with 25 nM CDDO-Im are shown. Values that are significantly different ($P < 0.05$) from that of the respective vehicle-treated controls (*) are indicated. Values are means plus standard errors (SEs) (error bars) ($n = 4$). (C) Response of wild-type and mutated *Ahr* promoter to ectopic expression of *Nrf2*ΔNeh2 (white bar) and mock plasmid (black bar). Values that are significantly different ($P < 0.05$) from that of the mock plasmid-transfected control (*) are indicated. Values are means plus SEs (error bars) ($n = 3$). (D) Binding of NRF2 to *Ahr* promoter in intact cells. Water (no DNA), inputs, chromatin immunoprecipitants with immunoglobulin G (IgG), and anti-NRF2 antibody (anti-NRF2) were used for PCR amplification of each promoter. (Top gel) ARE-containing promoter regions from the *Ahr* promoter were detected in NRF2 immunoprecipitants obtained from *Nrf2*$^{+/+}$ MEFs (+/+) but not from *Nrf2*$^{-/-}$ MEFs (−/−). (Bottom gel) Enhanced binding of NRF2 to the *Ahr* promoter following CDDO-Im (T) treatment compared to that in vehicle (V)-treated *Nrf2*$^{+/+}$ MEFs.

full-length promoter (p-967) was activated by CDDO-Im treatment (2.0-fold), as well as by forced expression of *Nrf2*ΔNeh2 (1.5-fold). This magnitude of response is consistent with the 2.1-fold increase in *Ahr* transcripts seen following treatment of wild-type MEFs with CDDO-Im (Fig. 1A). Responses to CDDO-Im were higher (2.6-fold) in proximal promoter constructs (p-242) than in the full-length promoter (Fig. 2B). These results suggest that a promoter containing 242 bp upstream of the transcription start site contains *cis* elements that can be activated by the NRF2-ARE. Further, when the upstream region containing the consensus ARE was deleted from the full-length promoter, the resulting construct (p-193) was not activated by CDDO-Im treatment (Fig. 2B). These results suggest that the −230 ARE may be necessary for the activation of the *Ahr* promoter by NRF2-ARE signaling. To confirm the results from promoter truncation, the −230 ARE was mutated in the p-967 and p-242 constructs (p-967mt and p-242mt [Fig. 2A]). This mutation in the ARE largely abolished promoter activation upon either CDDO-Im treatment (Fig. 2B) or *Nrf2*ΔNeh2 cotransfection in *Nrf2*$^{+/+}$ MEFs (Fig. 2C). These results indicate that the ARE is required for the activation of the promoter by NRF2. ChIP assays were performed to confirm that NRF2 binds to the *Ahr* promoter in intact cells. The promoter region containing an ARE at −230 bp was detected by PCR amplification with NRF2-immunoprecipitated chromatin from *Nrf2*$^{+/+}$ MEFs (Fig. 2D, top gel). As positive and negative controls, the ARE of the *Gsta1* promoter (10) was detected in NRF2-immunoprecipitated samples, whereas the β-*actin* promoter was not amplified. Levels of binding of NRF2 to the *Ahr* promoter were higher in CDDO-Im-treated cells than in vehicle-treated cells (Fig. 2D, bottom gel). A similar pattern of binding was observed with the *Gsta1* ARE. The *Gsta1* ARE and *Ahr* promoters were not amplified from *Nrf2*$^{-/-}$ MEFs. Collectively, these data suggest that NRF2 regulates transcription of *Ahr* through direct binding to the ARE in the *Ahr* promoter in both uninduced and induced states.

**Adipocyte differentiation was accelerated in *Nrf2*$^{-/-}$ MEFs.** As described above in the introduction, AHR inhibits conversion of 3T3-L1 preadipocytes and MEFs to mature lipid-containing adipocytes. Our findings show that immortalized *Nrf2*$^{-/-}$ MEFs have lower levels of AHR protein and mRNA, suggesting that NRF2 may influence adipogenesis via activation of AHR signaling. Therefore, the rate of adipogenesis of *Nrf2*$^{-/-}$ MEFs was compared to that of *Nrf2*$^{+/+}$ MEFs.

According to Alexander et al. (2), basal differentiation medium (containing insulin, dexamethasone, and isobutylmethylxanthine) used for preadipocyte differentiation was not sufficient to induce differentiation in immortalized MEF cell lines. Therefore, peroxisome proliferator-activated receptor gamma

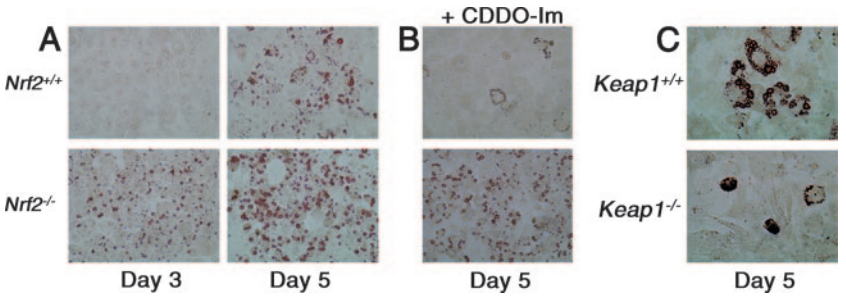


FIG. 3. Effects of *Nrf2* and *Keap1* genotypes on adipogenesis of MEFs. Cells were incubated with DMEM containing adipogenic reagents described in Materials and Methods. Representative photographs of the cells stained with Oil Red O are shown (400-fold magnified). (A) $Nrf2^{+/+}$ and $Nrf2^{-/-}$ MEFs 3 days and 5 days after stimulation of differentiation. (B) Effects of CDDO-Im (25 nM) on differentiation of $Nrf2^{+/+}$ and $Nrf2^{-/-}$ MEFs 5 days after stimulation of differentiation. (C) $Keap1^{+/+}$ and $Keap1^{-/-}$ MEFs 5 days after stimulation of differentiation.

(PPARγ) agonist rosiglitazone was added to the basal medium. Neither $Nrf2^{+/+}$ MEFs nor $Nrf2^{-/-}$ MEFs differentiate spontaneously to adipocytes (data not shown). However, lipid droplets were clearly detectable in immortalized $Nrf2^{-/-}$ MEFs 3 days after stimulation, whereas droplets were not visible until 5 days poststimulation in $Nrf2^{+/+}$ MEFs (Fig. 3A). CDDO-Im treatment substantially inhibited adipogenesis only in $Nrf2^{+/+}$ MEFs (Fig. 3B), further implying a negative role of NRF2 in adipogenesis.

Adipocyte differentiation is a process marked by a set of gene expression changes. CCAAT/enhancer-binding protein alpha (CEBPα) and PPARγ are transcription factors that regulate adipocyte-specific genes, such as fatty acid-binding proteins (FABPs) (14, 37, 47). Transcript levels of CEBPα and PPARγ are increased during differentiation, leading to upregulation of their downstream genes. Therefore, expression levels of CEBPα, PPARγ, and FABP4 serve as markers of adipocyte differentiation. Transcript levels of *Cebpα*, *Fabp4*, and *Pparγ2* were induced by stimulation with differentiation medium in both $Nrf2^{+/+}$ and $Nrf2^{-/-}$ MEFs (Fig. 4). Basal transcript levels of *Cebpα* and *Fabp4* were higher in $Nrf2^{-/-}$ MEFs than in $Nrf2^{+/+}$ MEFs (3.3-fold and 2.4-fold, respectively), and these higher levels were sustained throughout the differentiation process. No differences in the mRNA levels of *Pparγ2* between the two genotypes were detected. An increase in CEBPβ, which regulates transcription of PPARγ and CEBPα by binding to the CEBP response elements present in the promoter regions, is considered an early marker of adipogenesis (36). The basal transcript levels of this gene were lower in $Nrf2^{-/-}$ MEFs than in $Nrf2^{+/+}$ MEFs at day 0 and day 1, but not at later time points. Our data suggest that during differentiation, $Nrf2^{-/-}$ MEFs accumulate larger amounts of the terminal effectors, such as CEBPα and FABP4, that play important roles in both differentiation and lipid accumulation (14).

To determine whether the transcript levels and the actions (i.e., transactivation of downstream genes) of NRF2 and AHR are consistent with the adipogenesis pattern observed in Fig. 3, the mRNA levels of *Ahr*, *Nrf2* and downstream genes were monitored throughout the differentiation process (Fig. 4). The mRNA levels of *Nrf2* were not affected by differentiation (data not shown), but the mRNA levels of *Gsta1*, a marker of the action of NRF2, were lower in $Nrf2^{+/+}$ MEFs throughout differentiation, indicating that the transcriptional action of NRF2 is diminished during differentiation. Shimba et al. (40) reported that AHR was undetectable following adipogenesis in preadipocytes, and Alexander et al. (2) have shown that AHR was downregulated following adipogenesis in MEFs. Our data also confirmed that *Ahr* mRNA levels decrease during differentiation. A ChIP assay confirmed that NRF2 binding to the ARE at the −230 bp of *Ahr* promoter was suppressed 24 h after stimulation of differentiation (see Fig. S1 in the supplemental material). The basal levels of *Ahr* were lower in $Nrf2^{-/-}$

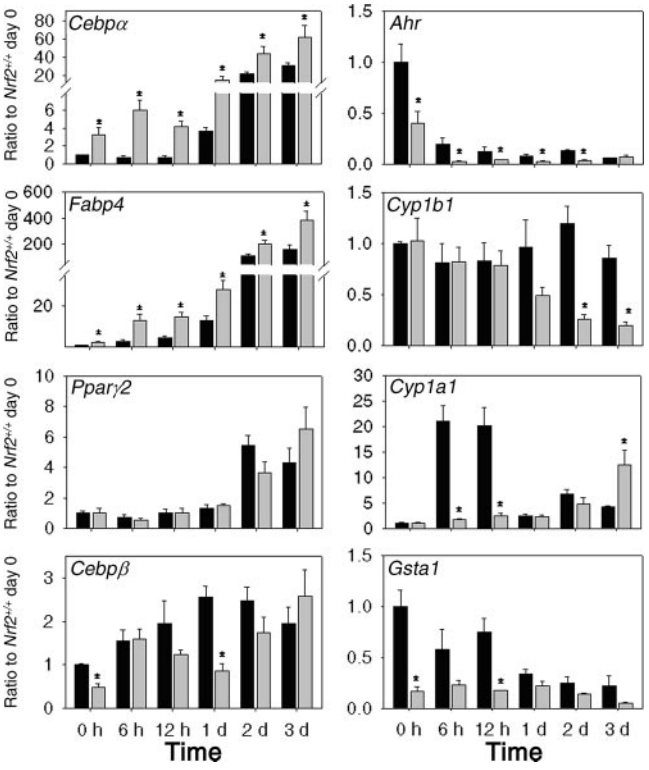


FIG. 4. Time-dependent changes of transcript levels throughout adipogenesis in $Nrf2^{+/+}$ MEFs (black bars) and $Nrf2^{-/-}$ MEFs (gray bars). Ratios to $Nrf2^{+/+}$ MEFs on day 0 (Ratio to $Nrf2^{+/+}$ day 0) are shown on the *y* axes. Time (in hours [h] and days [d]) is shown on the *x* axes. Values are means plus standard errors (error bars) ($n = 3$). Values that are significantly different ($P < 0.05$) from that of the respective $Nrf2^{+/+}$ MEFs (*) are indicated.

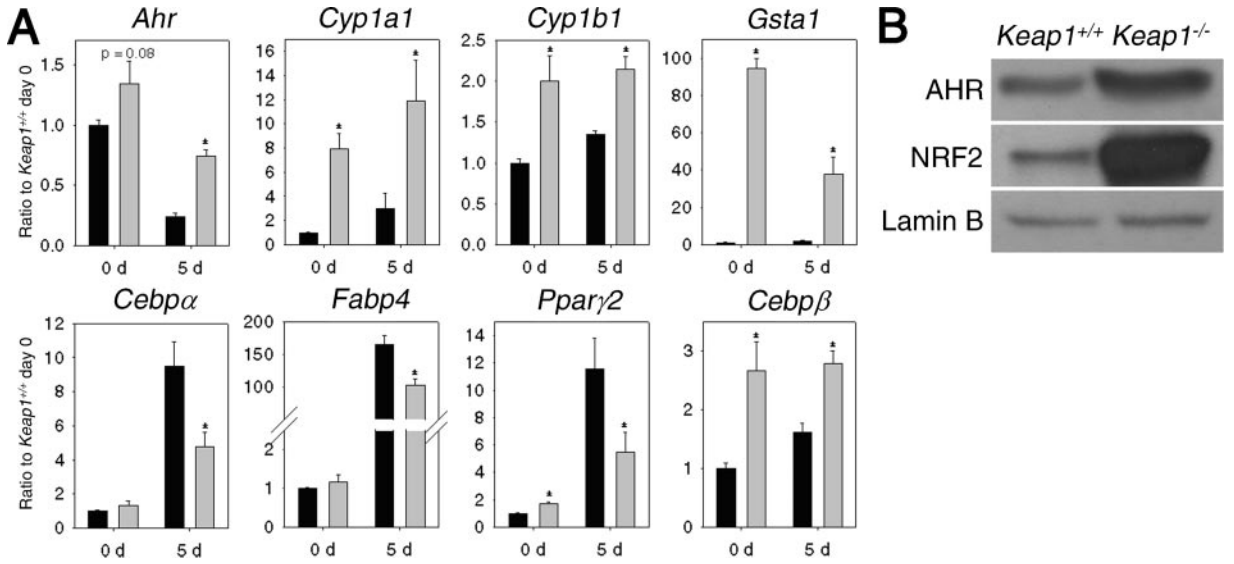


FIG. 5. Effects of *Keap1* genotype on transcript and protein levels in MEFs. (A) Transcript levels of *Ahr* and downstream genes and markers at day 0 and day 5 after stimulation of adipogenesis in $Keap1^{+/+}$ MEFs (black bars) and $Keap1^{-/-}$ MEFs (gray bars). Ratios to $Keap1^{+/+}$ MEFs on day 0 (Ratio to $Keap1^{+/+}$ day 0) are shown on the *y* axes. Time after stimulation of adipogenesis (in days [d]) is shown on the *x* axes. Values are means plus standard errors (error bars) ($n = 3$). Values that are significantly different ($P < 0.05$) from that of the respective $Keap1^{+/+}$ MEFs (*) are indicated. (B) Protein levels of AHR and NRF2 were detected by immunoblotting.

MEFs than in $Nrf2^{+/+}$ MEFs not only before stimulation (day 0) but also throughout the differentiation process. *Cyp1a1* and *Cyp1b1* mRNA levels were used as markers of AHR function. In $Nrf2^{+/+}$ MEFs, *Cyp1b1* mRNA levels were not affected by the treatment, whereas in $Nrf2^{-/-}$ MEFs, the levels started decreasing from day 1. *Cyp1a1* levels were markedly induced in $Nrf2^{+/+}$ MEFs at early time points but were relatively stable in $Nrf2^{-/-}$ MEFs. In summary, AHR expression and its downstream actions were decreased following adipogenesis and lower in $Nrf2^{-/-}$ MEFs than in $Nrf2^{+/+}$ MEFs. These data support our hypothesis that NRF2 acts as a negative regulator of adipogenesis through the regulation of *Ahr* transcription and signaling.

**Adipocyte differentiation was delayed in $Keap1^{-/-}$ MEFs.** To determine whether enhanced accumulation of NRF2 influences the rate of adipocyte differentiation, primary MEFs were established from a *Keap1*-disrupted mouse and a congenic wild-type mouse ($Keap1^{-/-}$ MEFs and $Keap1^{+/+}$ MEFs, respectively). After 5 days of adipocyte differentiation, lipid droplets were detectable both in primary $Keap1^{+/+}$ MEFs and $Keap1^{-/-}$ MEFs (Fig. 3C). However, the number of differentiated cells and size of the lipid droplets were substantially larger in $Keap1^{+/+}$ MEFs than in $Keap1^{-/-}$ MEFs. These results suggest that the enhanced NRF2 accumulation in $Keap1^{-/-}$ MEFs inhibits adipogenesis (after spontaneous immortalization, MEFs became smaller compared to primary cells; therefore, cells in Fig. 3C look bigger than cells in Fig. 3A).

The transcript levels of differentiation markers, *Ahr* and its downstream genes were detected at day 0 and day 5 after stimulation of adipogenesis in these cells (Fig. 5A). The mRNA levels of *Cebp*α, *Fabp4*, and *Pparγ2* were induced by stimulation with differentiation medium. The basal transcript levels of *Cebp*α and *Fabp4* were not affected by genotype at day 0 but were higher in $Keap1^{+/+}$ MEFs at day 5. The mRNA levels of *Pparγ2* were higher in $Keap1^{-/-}$ MEFs at day 0 but lower at day 5 compared to $Keap1^{+/+}$ MEFs. The mRNA levels of *Cebp*β were lower in $Keap1^{+/+}$ MEFs than in $Keap1^{-/-}$ MEFs, both at day 0 and day 5. These results suggest that increased NRF2 accumulation affects steps between inductions of *Cebp*β and *Cebp*α. These data are consistent with the pattern observed in Fig. 4. However, unlike the situation in immortalized $Nrf2^{+/+}$ and $Nrf2^{-/-}$ MEFs, *Pparγ2* may also play a role in primary MEFs.

Both transcript and protein levels of *Ahr* were increased by disruption of *Keap1* at day 0 (Fig. 5A and B), and transcript levels of *Ahr* were 3.1-fold higher in $Keap1^{-/-}$ MEFs than in $Keap1^{+/+}$ MEFs at day 5, suggesting that NRF2 regulates *Ahr* expression both before and during differentiation. The mRNA levels of *Cyp1a1* and *Cyp1b1* were not affected by adipogenesis but were higher in $Keap1^{+/+}$ MEFs at day 0 and day 5. These data suggest that NRF2 may affect not only *Ahr* transcription but also its function. *Gsta1* mRNA levels were decreased in $Keap1^{-/-}$ MEFs following adipogenesis but slightly increased in $Keap1^{+/+}$ MEFs. Overall, an inverse association between NRF2 accumulation and adipogenesis was observed, further confirming the inhibitory role of NRF2 in this process.

**Stable expression of *Ahr* and *Nrf2*ΔNeh2 rescued $Nrf2^{-/-}$ MEFs from adipocyte differentiation.** To determine whether ectopic expression of *Ahr* and *Nrf2* can "rescue" $Nrf2^{-/-}$ MEFs from differentiation, $Nrf2^{-/-}$ MEFs were transfected with mock vector or with plasmids expressing mouse *Ahr* and *Nrf2*ΔNeh2, and stable cell lines were established from these cells. At poststimulation day 3, mock transfectants showed accelerated lipid accumulation and morphological changes compared to cells expressing *Ahr* and *Nrf2*ΔNeh2 (Fig. 6A). The mRNA levels of *Fabp4* were substantially lower in *Ahr*- and *Nrf2*ΔNeh2-expressing cells than in control cells at day 3

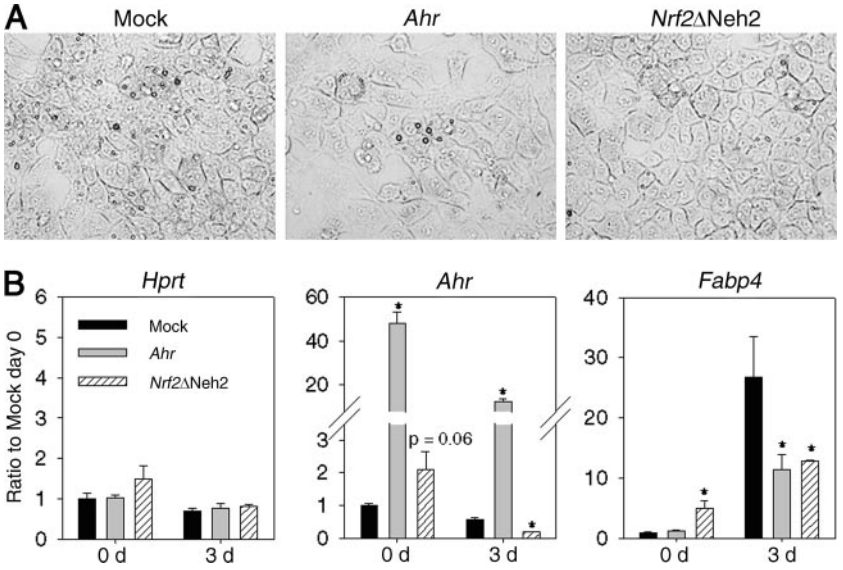


FIG. 6. Effects of ectopic expression of *Ahr* and *Nrf2*ΔNeh2 on adipogenesis of *Nrf2*$^{-/-}$ MEFs. (A) Representative photographs of the cells stained with Oil Red O and magnified 400-fold (3 days after stimulation of differentiation). (B) Transcript levels of *Hprt*, *Ahr*, and *Fabp4* at day 0 and day 3. The values for mock-transfected cells (black bars) and cells expressing *Ahr* (gray bars) and *Nrf2*ΔNeh2 (hatched bars) are shown. Ratios to mock transfectants at day 0 (Ratio to Mock day 0) are shown on the *y* axes. Time (in days [d]) is shown on the *x* axes. Values are means plus standard errors (error bars) ($n = 3$). Values that are significantly different ($P \leq 0.05$) from that of the respective mock transfectant (*) are indicated.

(Fig. 6B). The fact that mRNA levels of *Hprt* were not affected by stable transfection and differentiation shows that stable transfection does not influence nonspecific targets. mRNA levels of *Ahr* were elevated in *Ahr*- and *Nrf*ΔNeh2-expressing cells than in mock-transfected cells. However, the levels were significantly decreased in differentiated cells, suggesting that there are additional mechanisms that control *Ahr* gene transcription beside NRF2. The fact that the *Nrf2*ΔNeh2-expressing cells are more resistant to differentiation stimuli compared to mock-transfected cells excludes the possibilities that *Nrf2*$^{-/-}$ MEFs have differences other than *Nrf2* genotype that influence the phenotype. The finding that forced expression of *Ahr* rescued *Nrf2*$^{-/-}$ MEFs from adipogenesis provides direct support for our hypothesis that NRF2 inhibits adipogenesis through AHR signaling.

## DISCUSSION

Studying interactive networks between signaling pathways is indispensable for understanding the complexity of a phenotype. For example, several transcription factors have been implicated in the inflammatory process associated with asthma, including the glucocorticoid receptor, NF-κB, activator protein 1, nuclear factor of activated T-cells, cyclic AMP response element-binding protein, CEBP, PPAR, and NRF2 (38). Information on cross talk between signaling pathways may also provide insight into understanding the previously unrealized functions of a pathway and point to additional targets for interactions (11).

*Nrf2* gene transcription is directly modulated by AHR activation of XRE-like elements in the *Nrf2* promoter (27). NRF2 is also known to autoregulate its own expression through an ARE-like element in the proximal region of its promoter (22). However, this study is the first to show that NRF2 can affect *Ahr* transcription and downstream AHR signaling (Fig. 7). This bidirectional regulation of AHR and NRF2 pathways provides clues on the roles of NRF2 in complex diseases and in uncharacterized phenotypes.

The cross talk between NRF2 and AHR may help to explain the chemopreventive action of NRF2 activators. While studies on the AHR-CYP1A1 pathway often focus on production of toxic intermediates, the induction of both *CYP1A1* and *CYP1B1* resulted in an enhanced clearance of the procarcinogen benzo[*a*]pyrene (7). As suggested by Köhle and Bock (21), tightened coupling between the NRF2 and AHR pathways may result in attenuation of health risks caused by xenobiotics. The mode of action of bifunctional inducers, agents that enhance expression and activity of CYPs and cytoprotective enzymes (26), can be explained partially by our findings that NRF2 upregulates not only the expression of cytoprotective enzymes

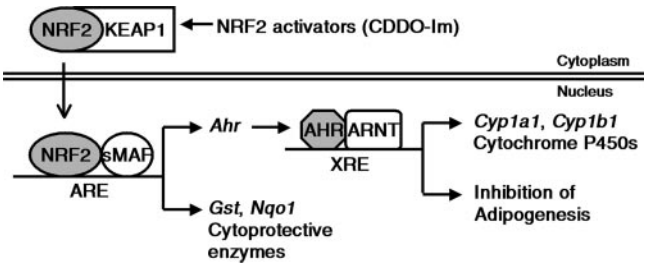


FIG. 7. Schematic representation of regulation of the AHR-XRE pathway by NRF2. The figure illustrates that interaction of NRF2 with ARE in the promoter of *Ahr* induces transcription of *Ahr* and triggers downstream events, the subsequent upregulation of cytochrome P450s and inhibition of adipogenesis. sMAF, small MAF proteins.

but also the expression of CYPs via AHR signaling. It is possible that drugs classified as bifunctional inducers increase expression of CYPs through NRF2-AHR-XRE interactions (Fig. 7).

Studies among various inbred strains of mice and $F_1$ hybrids have shown that inducibility of AHR-regulated enzymes is a function of the number of AHR molecules per cell (8). However, our studies do not indicate complete concordance between NRF2 levels, AHR levels, and AHR-regulated gene expression. Clearly, transcriptional upregulation of *Ahr* is one of the mechanisms by which NRF2 modulates AHR signaling. However, the 41% reduction of *Ahr* transcript levels in *Nrf2*$^{-/-}$ MEFs compared to *Nrf2*$^{+/+}$ MEFs may not be substantial enough to explain the complete abolishment of *Cyp1a1* and *Cyp1b1* induction by CDDO-Im in *Nrf2*$^{-/-}$ MEFs (Fig. 1A). Moreover, the transcript levels of *Ahr* were 1.3-fold higher in *Keap1*$^{-/-}$ MEFs than in *Keap1*$^{+/+}$ MEFs, while *Cyp1a1* and *Cyp1b1* mRNA levels were 7.9-fold and 2.0-fold higher in *Keap1*$^{-/-}$ MEFs, respectively (Fig. 5A). Immunoblots comparing *Keap1*$^{-/-}$ and *Nrf2*$^{-/-}$ MEFs to wild-type MEFs (Fig. 1D and 5B) imply that *Keap1* and *Nrf2* genotypes may also affect AHR expression in a posttranscriptional manner. Thus, it is possible that a minimal change in the level of *Ahr* mRNA is amplified during or after its translation.

Although the mRNA levels of *Cyp1a1* and *Cyp1b1* were analyzed as markers of transactivation by AHR and *Gsta1* as a marker of transactivation by NRF2, careful interpretation of the data is required. Isobutylmethylxanthine, which induces accumulation of cyclic AMP by inhibiting adenosine 3′,5′-cyclic monophosphate phosphodiesterase, was included in the differentiation medium. It is known that cyclic AMP activates AHR and induces its nuclear translocation (31). Dexamathasone, another component of the differentiation medium, potentiates induction of *Cyp1a1* transcription by TCDD (23). Our data suggest that the differentiation medium induced transcription of *Cyp1a1* in *Nrf2*$^{+/+}$ MEFs (Fig. 4). These data confirm that the activation of AHR-*Cyp1a1* signaling is dependent on *Nrf2* genotype because *Cyp1a1* transcription was not induced in *Nrf2*$^{-/-}$ MEFs. Transcript levels of *Cyp1b1* also did not correlate perfectly with the mRNA levels of *Ahr* (Fig. 4 and 5). This can be explained perhaps by the fact that *Cyp1b1* mRNA levels are regulated in an AHR-independent manner during adipogenesis (6). Our data show that *Gsta1* mRNA levels were decreased in *Nrf2*$^{+/+}$ MEFs and *Keap1*$^{-/-}$ MEFs throughout adipogenesis, suggesting that the action of NRF2 decreased during differentiation. However, it is possible that *Gsta1* transcripts also reflect diminished expression of AHR because it is well-known that GSTs are also induced by AHR agonists, such as TCDD (21, 48).

Data shown in Fig. S1 in the supplemental material suggest that NRF2 binding to the promoter of *Ahr* was decreased during adipocyte differentiation. However, RT-PCR data confirmed that *Ahr* transcription was suppressed from 6 h after stimulation of differentiation (Fig. 4), while the change in NRF2 binding to ARE was detectable only after 24 h. Furthermore, *Ahr* mRNA levels were affected in *Nrf2*$^{-/-}$ MEFs and *Nrf2*$^{+/+}$ MEFs. These results suggest that NRF2 is not the only factor that controls *Ahr* gene transcription during adipocyte differentiation. Indeed, our results are consistent with the report of Shimba et al. (40) demonstrating that the sequence of the *Ahr* promoter region responsible for differentiation-dependent suppression of *Ahr* transcription does not contain an ARE. Our findings also suggest that the level of expression of *Ahr* before stimulation of differentiation might be more important for determination of cell fate than transcriptional regulation during adipogenesis, since suppression of *Ahr* transcription was observed in *Nrf2*$^{-/-}$ MEFs and *Nrf2*$^{+/+}$ MEFs (Fig. 4) and in mock-transfected cells and *Nrf2*ΔNeh2-transfected cells (Fig. 6).

In addition to regulation of expression of CYPs, AHR plays a role in a number of processes, such as development, apoptosis, growth, and adipogenesis (34, 49, 52). Among these AHR-dependent phenotypes, our work evaluated the role of NRF2 on regulation of adipogenesis because of the central role of adipogenesis in multiple diseases, such as obesity (a major risk factor for diabetes, cancer, and cardiovascular diseases) and lipodystrophy (5, 16, 35). Various in vitro models for adipogenesis, such as embryonic stem cells, preadipocytes, and MEFs, are available (4). Among these models, adipogenesis using MEFs is particularly useful to study the effects of gene knockouts. The fact that disruption of *Nrf2* accelerated differentiation to adipocytes, while disruption of *Keap1* delayed the process (Fig. 3A and C) implies a negative role of NRF2 in adipogenesis. Pharmacological targeting of the NRF2 pathway with CDDO-Im, which inhibited differentiation (Fig. 3B), confirmed that NRF2 modulates components of adipocyte differentiation.

To evaluate how NRF2 regulates adipogenesis, differentiation markers involved at multiple stages of adipogenesis were analyzed. CEBPs and PPARs are the two families of transcription factors that play critical roles in adipogenesis (47). CEBPβ and CEBPδ function at an early phase of the differentiation process by sensing adipogenic stimuli and initiating expression of CEBPα and PPARγ (37, 47). CEBPα and PPARγ play roles at a later stage by inducing and maintaining expression of adipocyte-specific genes, such as *Fabp4* (14). The elevation of CEBPβ upon adipogenic stimulation is transient, while CEBPα and PPARγ remain upregulated for the duration of adipogenesis (43).

Although the mechanism by which AHR regulates adipogenesis has not been fully characterized, recent work suggests that AHR affects differentiation stages that follow CEBPβ activation, i.e., CEBPα or PPARγ upregulation. In 3T3-L1 preadipocytes, forced expression of AHR resulted in lower induction of *Fabp4* and *Cebp*α upon differentiation than in control cells, while the induction of *Ppar*γ was not affected (41). *Ppar*γ expression could be induced by differentiation in *Ahr*$^{-/-}$ MEFs, but levels were lower than in *Ahr*$^{+/+}$ MEFs (2). In addition, Vogel and Matsumura (45) demonstrated that although TCDD suppressed adipogenesis of MEFs, it induced expression of *Cebp*β rather than inhibiting it.

In the present study, mRNA levels of *Cebp*α and *Fabp4* were higher in *Nrf2*$^{-/-}$ MEFs than in *Nrf2*$^{+/+}$ MEFs both before and after differentiation, while induction of *Ppar*γ*2* was not affected by *Nrf2* genotype (Fig. 4). mRNA levels of *Cebp*β were lower in *Nrf2*$^{-/-}$ MEFs than in *Nrf2*$^{+/+}$ MEFs. In primary *Keap1*$^{-/-}$ MEFs (Fig. 5A), disruption of *Keap1* (which leads to accumulation of NRF2 in the nucleus) resulted in minimal induction of *Cebp*α, *Fabp4*, and *Ppar*γ*2* upon differentiation. *Cebp*β mRNA levels remained higher in *Keap1*$^{-/-}$ MEFs than

in *Keap1*$^{+/+}$ MEFs, both before and after induction of adipogenesis. These data suggest that NRF2 negatively modulates expression of *Cebp*α and *Ppar*γ*2* but not *Cebp*β during the course of adipogenesis. The stages of differentiation that are affected by NRF2 directly overlap with those affected by AHR, thereby supporting the hypothesis that NRF2 inhibits adipogenesis through cross talk with AHR signaling.

Although how AHR controls expression of XRE genes has been extensively studied, the molecular events that regulate *Ahr* expression itself have been less well investigated (40). Our findings represent a new perspective for control of *Ahr* expression by demonstrating that NRF2 directly binds to a functional ARE found in the proximal promoter of *Ahr* (Fig. 2). Our data also suggest that NRF2 affects AHR function (i.e., transcription of *Cyp1a1* and *Cyp1b1* and adipogenesis) in an exogenous ligand-independent manner. Tijet et al. (44) identified a number of genes for which expression is AHR dependent but TCDD independent, suggesting that the constitutive level of AHR may affect gene expression. Candidates for endogenous AHR ligand, such as indigo (42), may also play a role in the interaction with the NRF2 pathway.

In summary, the observation that NRF2 controls AHR signaling expands the function of NRF2 to include influencing the metabolism of xenobiotics and carcinogens via CYPs as well as controlling adipogenesis. Recent studies of *Ahr Nrf2* double knockout mice in comparisons with wild-type and single transcription factor knockout mice offer additional evidence for interactions between these pathways (30). Although not addressed experimentally in this report, our findings also imply that the modifying influence of the NRF2 pathway can be expanded to other AHR-dependent processes, such as programmed cell death and development. Moreover, our findings may allow a broader clinical application of NRF2 activators, such as in prevention and treatment of obesity.

## ACKNOWLEDGMENTS

This work was supported by NIH grants CA94076, HL081205, and ES03819. S. Shin is the recipient of a Samsung Scholarship (Samsung Foundation of Culture).

We thank K. N. Anuzis (Johns Hopkins University) for help with adipocyte differentiation, A. Singh (Johns Hopkins University) and M. K. Kwak (Yeungnam University) for help with the ChIP assay. We also thank K. Itoh (Hirosaki University), Y. Fujii-Kuriyama, and J. Mimura (University of Tsukuba) for providing anti-NRF2 antibody and *Nrf2*ΔNeh2-expression plasmid and M. B. Sporn (Dartmouth Medical School) for providing CDDO-Im.

## REFERENCES

1. **Alexander, D. L., S. E. Eltom, and C. R. Jefcoate.** 1997. Ah receptor regulation of CYP1B1 expression in primary mouse embryo-derived cells. Cancer Res. **57:**4498–4506.
2. **Alexander, D. L., L. G. Ganem, P. Fernandez-Salguero, F. Gonzalez, and C. R. Jefcoate.** 1998. Aryl-hydrocarbon receptor is an inhibitory regulator of lipid synthesis and of commitment to adipogenesis. J. Cell Sci. **111:**3311–3322.
3. **Boone, C., H. Bussey, and B. J. Andrews.** 2007. Exploring genetic interactions and networks with yeast. Nat. Rev. Genet. **8:**437–449.
4. **Bost, F., M. Aouadi, L. Caron, and B. Binetruy.** 2005. The role of MAPKs in adipocyte differentiation and obesity. Biochimie **87:**51–56.
5. **Camp, H. S., D. Ren, and T. Leff.** 2002. Adipogenesis and fat-cell function in obesity and diabetes. Trends. Mol. Med. **8:**442–447.
6. **Cho, Y. C., W. Zheng, M. Yamamoto, X. Liu, P. R. Hanlon, and C. R. Jefcoate.** 2005. Differentiation of pluripotent C3H10T1/2 cells rapidly elevates CYP1B1 through a novel process that overcomes a loss of Ah receptor. Arch. Biochem. Biophys. **439:**139–153.
7. **Ebert, B., A. Seidel, and A. Lampen.** 2005. Induction of phase-1 metabolizing enzymes by oltipraz, flavone and indole-3-carbinol enhance the formation and transport of benzo[a]pyrene sulfate conjugates in intestinal Caco-2 cells. Toxicol. Lett. **158:**140–151.
8. **Eisen, H. J., R. R. Hannah, C. L. Legraverend, A. B. Okey, and D. W. Nebert.** 1983. The Ah receptor: controlling factor in the induction of drug-metabolizing enzymes by certain chemical carcinogens and other environmental pollutants, p. 227–258. *In* G. Litwack (ed.), Biochemical actions of hormones, vol. 10. Academic Press, New York, NY.
9. **Fong, C. J., L. D. Burgoon, and T. R. Zacharewski.** 2005. Comparative microarray analysis of basal gene expression in mouse Hepa-1c1c7 wild-type and mutant cell lines. Toxicol. Sci. **6:**342–353.
10. **Friling, R. S., A. Bensimon, Y. Tichauer, and V. Daniel.** 1990. Xenobiotic-inducible expression of murine glutathione S-transferase Ya subunit gene is controlled by an electrophile-responsive element. Proc. Natl. Acad. Sci. USA **87:**6258–6262.
11. **Gianchandani, E. P., D. L. Brautigan, and J. A. Papin.** 2006. Systems analyses characterize integrated functions of biochemical networks. Trends Biochem. Sci. **31:**284–291.
12. **Goldring, C., N. Kitteringham, R. Jenkins, I. Copple, J. F. Jeannin, and B. K. Park.** 2006. Plasticity in cell defence: access to and reactivity of critical protein residues and DNA response elements. J. Exp. Biol. **209:**2337–2343.
13. **Gouédard, C., R. Barouki, and Y. Morel.** 2004. Dietary polyphenols increase paraoxonase 1 gene expression by an aryl hydrocarbon receptor-dependent mechanism. Mol. Cell. Biol. **24:**5209–5222.
14. **Gregoire, F. M., C. M. Smas, and H. S. Sul.** 1998. Understanding adipocyte differentiation. Physiol. Rev. **78:**783–809.
15. **Hankinson, O.** 2005. Role of coactivators in transcriptional activation by the aryl hydrocarbon receptor. Arch. Biochem. Biophys. **433:**379–386.
16. **Harp, J. B.** 2004. New insights into inhibitors of adipogenesis. Curr. Opin. Lipidol. **15:**303–307.
17. **Itoh, K., N. Wakabayashi, Y. Katoh, T. Ishii, K. Igarashi, J. D. Engel, and M. Yamamoto.** 1999. Keap1 represses nuclear activation of antioxidant responsive elements by Nrf2 through binding to the amino-terminal Neh2 domain. Genes Dev. **13:**76–86.
18. **Kensler, T. W., N. Wakabayashi, and S. Biswal.** 2007. Cell survival responses to environmental stresses via the Keap1-Nrf2-ARE pathway. Annu. Rev. Pharmacol. Toxicol. **47:**89–116.
19. **Kobayashi, A., M. I. Kang, Y. Watai, K. I. Tong, T. Shibata, K. Uchida, and M. Yamamoto.** 2006. Oxidative and electrophilic stresses activate Nrf2 through inhibition of ubiquitination activity of Keap1. Mol. Cell. Biol. **26:**221–229.
20. **Köhle, C., and K. W. Bock.** 2006. Activation of coupled Ah receptor and Nrf2 gene batteries by dietary phytochemicals in relation to chemoprevention. Biochem. Pharmacol. **72:**795–805.
21. **Köhle, C., and K. W. Bock.** 2007. Coordinate regulation of phase I and II xenobiotic metabolisms by the Ah receptor and Nrf2. Biochem. Pharmacol. **73:**1853–1862.
22. **Kwak, M. K., K. Itoh, M. Yamamoto, and T. W. Kensler.** 2002. Enhanced expression of the transcription factor Nrf2 by cancer chemopreventive agents: role of antioxidant response element-like sequences in the *nrf2* promoter. Mol. Cell. Biol. **22:**2883–2892.
23. **Lai, K. P., M. H. Wong, and C. K. Wong.** 2004. Modulation of AhR-mediated CYP1A1 mRNA and EROD activities by 17beta-estradiol and dexamethasone in TCDD-induced H411E cells. Toxicol. Sci. **78:**41–49.
24. **Loose, M., and R. Patient.** 2006. Global genetic regulatory networks controlling hematopoietic cell fates. Curr. Opin. Hematol. **13:**229–236.
25. **Ma, Q., K. Kinneer, Y. Bi, J. Y. Chan, and Y. W. Kan.** 2004. Induction of murine NAD(P)H:quinone oxidoreductase by 2,3,7,8-tetrachlorodibenzo-p-dioxin requires the CNC (cap 'n' collar) basic leucine zipper transcription factor Nrf2 (nuclear factor erythroid 2-related factor 2): cross-interaction between AhR (aryl hydrocarbon receptor) and Nrf2 signal transduction. Biochem. J. **377:**205–213.
26. **Miao, W., L. Hu, M. Kandouz, D. Hamilton, and G. Batist.** 2004. A cell-based system to identify and characterize the molecular mechanism of drug-metabolizing enzyme (DME) modulators. Biochem. Pharmacol. **67:**1897–1905.
27. **Miao, W., L. Hu, P. J. Scrivens, and G. Batist.** 2005. Transcriptional regulation of NF-E2 p45-related factor (NRF2) expression by the aryl hydrocarbon receptor-xenobiotic response element signaling pathway: direct cross-talk between phase I and II drug-metabolizing enzymes. J. Biol. Chem. **280:**20340–20348.
28. **Nakata, K., Y. Tanaka, T. Nakano, T. Adachi, H. Tanaka, T. Kaminuma, and T. Ishikawa.** 2006. Nuclear receptor-mediated transcriptional regulation in phase I, II, and III xenobiotic metabolizing systems. Drug Metab. Pharmacokinet. **21:**437–547.
29. **Nebert, D. W., A. L. Roe, M. Z. Dieter, W. A. Solis, Y. Yang, and T. P. Dalton.** 2000. Role of the aromatic hydrocarbon receptor and [Ah] gene battery in the oxidative stress response, cell cycle control, and apoptosis. Biochem. Pharmacol. **59:**65–85.
30. **Noda, S., N. Harada, A. Hida, Y. Fujii-Kuriyama, H. Motohashi, and M. Yamamoto.** 2003. Gene expression of detoxifying enzymes in AhR and Nrf2

compound null mutant mouse. Biochem. Biophys. Res. Commun. **303:**105–111.

31. **Oesch-Bartlomowicz, B., A. Huelster, O. Wiss, P. Antoniou-Lipfert, C. Dietrich, M. Arand, C. Weiss, E. Bockamp, and F. Oesch.** 2005. Aryl hydrocarbon receptor activation by cAMP vs. dioxin: divergent signaling pathways. Proc. Natl. Acad. Sci. USA **102:**9218–9223.
32. **Okawa, H., H. Motohashi, A. Kobayashi, H. Aburatani, T. W. Kensler, and M. Yamamoto.** 2006. Hepatocyte-specific deletion of the keap1 gene activates Nrf2 and confers potent resistance against acute drug toxicity. Biochem. Biophys. Res. Commun. **339:**79–88.
33. **Pfaffl, M. W.** 2001. A new mathematical model for relative quantification in real-time RT-PCR. Nucleic Acids Res. **29:**e45.
34. **Puga, A., C. R. Tomlinson, and Y. Xia.** 2005. Ah receptor signals cross-talk with multiple developmental pathways. Biochem. Pharmacol. **69:**199–207.
35. **Rodriguez, A., A. Duran, M. Selloum, M. F. Champy, F. J. Diez-Guerra, J. M. Flores, M. Serrano, J. Auwerx, M. T. Diaz-Meco, and J. Moscat.** 2006. Mature-onset obesity and insulin resistance in mice deficient in the signaling adapter p62. Cell Metab. **3:**211–222.
36. **Rosen, E. D., C. J. Walkey, P. Puigserver, and B. M. Spiegelman.** 2000. Transcriptional regulation of adipogenesis. Genes Dev. **14:**1293–1307.
37. **Rosen, E. D.** 2005. The transcriptional basis of adipocyte development. Prostaglandins Leukot. Essent. Fatty Acids **73:**31–34.
38. **Roth, M., and J. L. Black.** 2006. Transcription factors in asthma: are transcription factors a new target for asthma therapy? Curr. Drug Targets **7:**589–595.
39. **Schmidt, J. V., G. H. Su, J. K. Reddy, M. C. Simon, and C. A. Bradfield.** 1996. Characterization of a murine Ahr null allele: involvement of the Ah receptor in hepatic growth and development. Proc. Natl. Acad. Sci. USA **93:**6731–6736.
40. **Shimba, S., M. Hayashi, T. Ohno, and M. Tezuka.** 2003. Transcriptional regulation of the AhR gene during adipose differentiation. Biol. Pharm. Bull. **26:**1266–1271.
41. **Shimba, S., T. Wada, and M. Tezuka.** 2001. Arylhydrocarbon receptor (AhR) is involved in negative regulation of adipose differentiation in 3T3-L1 cells: AhR inhibits adipose differentiation independently of dioxin. J. Cell Sci. **114:**2809–2817.
42. **Sugihara, K., S. Kitamura, T. Yamada, T. Okayama, S. Ohta, K. Yamashita, M. Yasuda, Y. Fujii-Kuriyama, K. Saeki, S. Matsui, and T. Matsuda.** 2004. Aryl hydrocarbon receptor-mediated induction of microsomal drug-metabolizing enzyme activity by indirubin and indigo. Biochem. Biophys. Res. Commun. **318:**571–578.
43. **Tang, Q. Q., J. W. Zhang, and M. D. Lane.** 2004. Sequential gene promoter interactions of C/EBPbeta, C/EBPalpha, and PPARgamma during adipogenesis. Biochem. Biophys. Res. Commun. **319:**235–239.
44. **Tijet, N., P. C. Boutros, I. D. Moffat, A. B. Okey, J. Tuomisto, and R. Pohjanvirta.** 2006. Aryl hydrocarbon receptor regulates distinct dioxin-dependent and dioxin-independent gene batteries. Mol. Pharmacol. **69:**140–153.
45. **Vogel, C. F., and F. Matsumura.** 2003. Interaction of 2,3,7,8-tetrachlorodibenzo-p-dioxin (TCDD) with induced adipocyte differentiation in mouse embryonic fibroblasts (MEFs) involves tyrosine kinase c-Src. Biochem. Pharmacol. **66:**1231–1244.
46. **Wakabayashi, N., K. Itoh, J. Wakabayashi, H. Motohashi, S. Noda, S. Takahashi, S. Imakado, T. Kotsuji, F. Otsuka, D. R. Roop, T. Harada, J. D. Engel, and M. Yamamoto.** 2003. Keap1-null mutation leads to postnatal lethality due to constitutive Nrf2 activation. Nat. Genet. **35:**238–245.
47. **Wu, Z., N. L. Bucher, and S. R. Farmer.** 1996. Induction of peroxisome proliferator-activated receptor γ during the conversion of 3T3 fibroblasts into adipocytes is mediated by C/EBPβ, C/EBPδ, and glucocorticoids. Mol. Cell. Biol. **16:**4128–4136.
48. **Xiao, G. H., J. A. Pinaire, A. D. Rodrigues, and R. A. Prough.** 1995. Regulation of the Ah gene battery via Ah receptor-dependent and independent processes in cultured adult rat hepatocytes. Drug Metab. Dispos. **23:**642–650.
49. **Yang, X., D. Liu, T. J. Murray, G. C. Mitchell, E. V. Hesterman, S. I. Karchner, R. R. Merson, M. E. Hahn, and D. H. Sherr.** 2005. The aryl hydrocarbon receptor constitutively represses c-myc transcription in human mammary tumor cells. Oncogene **24:**7869–7881.
50. **Yates, M. S., and T. W. Kensler.** 2007. Chemopreventive promise of targeting the Nrf2 pathway. Drug News Perspect. **20:**109–117.
51. **Yates, M. S., M. Tauchi, F. Katsuoka, K. C. Flanders, K. T. Liby, T. Honda, G. W. Gribble, D. A. Johnson, J. A. Johnson, N. C. Burton, T. R. Guilarte, M. Yamamoto, M. B. Sporn, and T. W. Kensler.** 2007. Pharmacodynamic characterization of chemopreventive triterpenoids as exceptionally potent inducers of Nrf2-regulated genes. Mol. Cancer Ther. **6:**154–162.
52. **Zaher, H., P. M. Fernandez-Salguero, J. Letterio, M. S. Sheikh, A. J. Fornace, Jr., A. B. Roberts, and F. J. Gonzalez.** 1998. The involvement of aryl hydrocarbon receptor in the activation of transforming growth factor-beta and apoptosis. Mol. Pharmacol. **54:**313–321.